



ELSEVIER

Available at

www.ElsevierComputerScience.com

POWERED BY SCIENCE @ DIRECT®

Pattern Recognition Letters 24 (2003) 2995–3006

Pattern Recognition
Letters

www.elsevier.com/locate/patrec

Fast image segmentation based on multi-resolution analysis and wavelets

Byung-Gyu Kim ^{*}, Jae-Ick Shim, Dong-Jo Park

*Department of Electrical Engineering and Computer Science, Korea Advanced Institute of Science and Technology,
373-1 Guseong-dong, Yuseong-gu, Daejeon, South Korea*

Received 4 December 2002; received in revised form 11 June 2003

Abstract

An efficient algorithm for image segmentation based on a multi-resolution application of a wavelets transform and feature distribution is presented. The original feature space is transformed into a lower resolution with a wavelets transform to derive fast computation of the optimum threshold value in a feature space. Based on this lower resolution version of the given feature space, a single feature value or multiple feature values are determined as the optimum threshold values. The optimum feature values, which are in the lower resolution, are projected onto the original feature space. In this step a refinement procedure may be added to detect the optimum threshold value. Experimental results for the proposed algorithm indicate feasibility and reliability for fast image segmentation.

© 2003 Elsevier B.V. All rights reserved.

Keywords: Multi-resolution analysis; Image segmentation; Wavelets transform; Feature space; Multi-threshold

1. Introduction

Image segmentation plays an important role in computer vision and image processing to interpret and analyze an acquired image. Separation of objects or image regions is usually required for high-level image comprehension in practical applications involving visual inspection. Thresholding based on a feature distribution is widely used to segment the desired image into several image regions because of the simplicity and ability of real-time implementation.

Various kinds of thresholding techniques have been proposed over the years, most of which require optimization of a criterion function. Thresholding for image segmentation is usually performed based on information contained in a grey level histogram of a given image. The objective of this approach is to locate the bottom of the valley of the histogram that, hopefully, best separates the two groups or segments. Parametric and non-parametric approaches have been used to locate the bottom of the valley of the histogram. In the parametric approach, a model is assumed to have the probability density function of the grey level distribution of each group, which is assumed to be Gaussian. One then attempts to find estimates of the parameters of the distribution using the given

^{*} Corresponding author.

E-mail address: chitos@mail.kaist.ac.kr (B.-G. Kim).

histogram. The bottom of the valley is obtained from these estimates (Kittler and Illingworth, 1986; Kumar et al., 1995). These estimates are often not useful when the mismatch between the real distribution and assumed model is too large.

In the non-parametric approach, we are interested in separating two grey level distributions in an optimum manner according to a criterion, such as within-class variance, between-class variance, total variance, or entropy (Kittler and Illingworth, 1986; Kumar et al., 1995; Calvard, 1978; Otsu, 1979; Pun, 1981; Abutaleb, 1989). Calvard (1978) has presented an iterative threshold selection method for separating an object when the histogram of the image is bi-modal. Otsu (1979) has proposed a method that selects an optimum threshold value using a discriminant criterion that maximizes the separation of the resultant classes in grey levels.

Entropic thresholding was suggested by Pun (1981) and Cao et al. (2002). This method selects an optimum threshold value that maximizes a posterior entropy H' of the gray level histogram. Abutaleb used two dimensional entropic thresholding with the histogram and spatial information of an image (Abutaleb, 1989; Wu et al., 1999).

Most methods search for the optimum threshold values on the basis of a criterion in the feature space. Generally, the search time for the optimum feature value increases as the dimension of the feature space increases, and vice versa. Therefore, it is necessary to develop a technique for dimension reduction of the original feature space.

Multi-resolution approaches are usually used for dimension reduction of image data (Salgado et al., 2000). A wavelets transform is an especially efficient tool for data approximation, compression, and noise removal (Walker, 1999; Goswami and Chan, 1999). Shi and Shibasaki (1999) used wavelets for detection of edges. Other methods have been devised for color texture segmentation in the wavelets domain since the characteristics of the direction and frequency of texture can be easily identified (Liapis et al., 2000; Noda et al., 2000; Acharyya and Kundu, 2001; Zhang and Oe, 1998; Charalampidis and Kasparis, 2002).

We propose a fast scheme for partitioning an image based on the feature distribution and multi-

resolution analysis. The gray scale intensity is considered as a feature for image segmentation. However, our method can be applied to any feature distribution that should be separated. The intensity distribution for a given image is first generated. Then, this distribution is transformed into a lower resolution using the wavelets transform. The original signal in the wavelets theory is decomposed into two signals at the next lower level (Walker, 1999; Goswami and Chan, 1999). One signal is the trend or approximation signal while the other signal is the detailed signal. At the lower level, the approximation signal gives the dimension-reduced version of the original signal while it contains the overall characteristics of the original signal. Using this dimension reduced version, the optimum feature values are selected in the lower level. Finally, the optimum feature values are expanded into the original feature space.

This paper is organized as follows: We describe multi-resolution analysis (MRA) and a wavelets transform in Section 2 where the fast technique for image segmentation is developed in detail. Section 3 deals with testing results for the proposed algorithm on several images and gives results of the segmentation. Conclusions are presented in Section 4.

2. Fast image segmentation based on multi-resolution analysis

2.1. Multi-resolution analysis (MRA) and wavelets transform

Multi-resolution analysis (MRA) is often used for signal representations and signal processing because it can represent signals at the split resolution and scale space. In multi-resolution analysis, a signal is viewed at various levels of approximations or resolutions. A complicated signal is divided into several simpler signals by applying MRA, and each signal is considered separately.

From the viewpoint of signal spaces, the multi-resolution spaces can be represented as the following relations:

$$A_m \cap W_m = \{0\}, \quad m \in Z, \quad (1)$$

$$A_{m+1} \oplus W_{m+1} = A_m, \tag{2}$$

where m denotes the index of scales or resolutions. For each m , A_{m+1} is a proper subspace of A_m and there is some space left in A_m , called W_{m+1} , which when combined with A_{m+1} gives A_m .

With the condition Eq. (1), the summation in Eq. (2) is referred as *direct sum* and decomposition in Eq. (2) as a *direct-sum decomposition* in (Goswami and Chan, 1999). The following relation is satisfied by Eq. (2):

$$\begin{aligned} A_{m+1} &= A_{m+2} \oplus W_{m+2} = W_{m+2} \oplus W_{m+3} \oplus A_{m+3} \\ &= W_{m+2} \oplus W_{m+3} \oplus W_{m+4} \oplus \dots \end{aligned} \tag{3}$$

Fig. 1 shows a diagram representation of the hierarchical nature of A_m and W_m as the above relationships.

In wavelets theory, subspaces $\{W_m\}$ are generated by $\psi(t) \in L^2_R$, called the *wavelets*. Subspaces $\{A_m\}$ are generated by $\phi(t) \in L^2(R)$, called a *scaling function*, in the same way. The trend of a given signal is approximated by the scaling function and the detailed fluctuation is extracted by the wavelets signal. Thus, the transformed signals in subspaces $\{A_m\}$ are approximations of the original and those in $\{W_m\}$ are the details of that. The transformed signals can be perfectly converted to the original signals.

2.2. The proposed algorithm for fast image segmentation

A wavelets transform divides a signal into several simpler signals at a different scale and can significantly reduce the dimension of the signal as the level of the transform increases. However, the overall characteristic of the original signal can be approximated. Our method makes use of a wavelets transform to select the proper threshold values in a given feature distribution.

Let the gray level be the defined feature and $h(k)$ be the original distribution of a given image. The proposed algorithm is then composed of four main steps as follows:

(1) With the original distribution $h(k)$, the wavelet transform with a level m is performed by decimation operation by 2^m after the convolution of the original distribution $h(k)$ with $\psi(t)$ and $\phi(t)$. $h^m(l) = WT^m[h(k)]$, $m \in Z = h^m_A(l) + h^m_W(l)$, (4)

where $h^m_A(l)$ is the trend of the original distribution and $h^m_W(l)$ is the details of that in the m th level. For any trend signal in the level m , this is decomposed into the dimension-reduced two signals in the level $m + 1$, successively:

$$h^m_A(l) = h^{m+1}_A(l) + h^{m+1}_W(l). \tag{5}$$

(2) Using the trend signal $h^m_A(l)$ at the lower resolution m , proper threshold values, θ^m_i

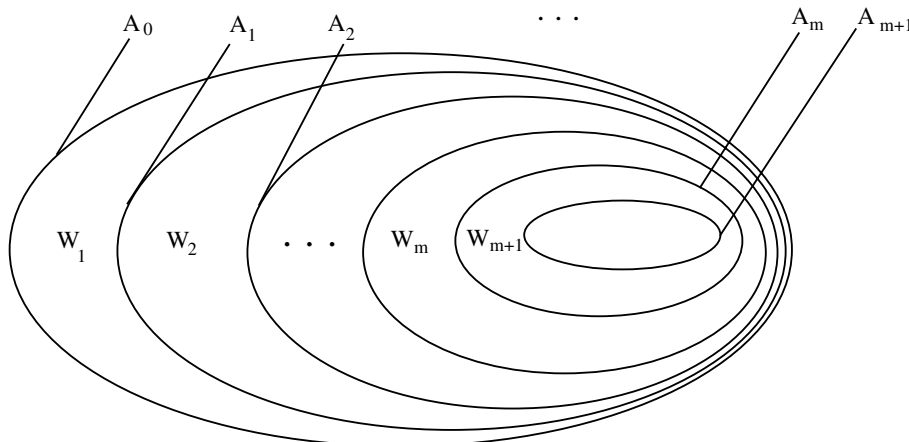


Fig. 1. Subspaces in MRA.

($i = 1, \dots, L$) are determined by some discriminant function such as Otsu’s separability, the entropy-based discrepancy and so on, where L denotes the number of the desired threshold values. Since dimension of the trend signal $h_A^m(l)$ at the level m is very low, the consumed time for searching the threshold values θ_i^m is significantly decreased.

(3) The selected θ_i^m in level m are expanded to the original space $h(k)$. In our method, two expansion modes are used including (1) direct expansion and (2) refinement after the direct expansion.

The wavelets transform with the level m can be performed by a decimation operation by 2^m after the convolution of the original signal with wavelets $\psi(t)$ and scaling function $\phi(t)$. Therefore, to obtain the proper values in the original signal space, it is reasonable to expand for an approximation of the range of the original space by multiplying the trend signal of the m th lower level space by a factor of 2^m .

In the direct expansion mode, the final threshold values θ_i is acquired by multiplying a factor of 2^m as follow:

$$\theta_i = \hat{\theta}_i = \theta_i^m \times 2^m, \quad \text{for } i = 1, \dots, L, \quad (6)$$

A refinement procedure can be added to obtain more accurate threshold values. In this mode, the direct expansion is first performed by Eq. (6) at first. Then, the final optimum values are located in a very small range around the expanded values of the original space For the i th direct expansion value $\hat{\theta}_i$,

$$\theta_i = \max_{\theta \in [\hat{\theta}_i - \theta_{\text{var}}, \hat{\theta}_i + \theta_{\text{var}}]} F(\theta), \quad (7)$$

where $F(\theta)$ is the discriminant function which is used for segmentation and θ_{var} is the predefined dynamic range for refinement procedure. If we utilize the other discriminant function that should be minimized, the final optimal values are determined for the minima of Eq. (7). In our study, θ_{var} is fixed as 4 for all experiments. Also, Otsu’s (1979) separability ($\sigma_B^2(\theta)$) is used as the discriminant function $F(\theta)$ to select the optimum threshold values θ_i based on the gray level distribution. In Otsu’s method for the bi-level thresholding, the separability (or goodness) of the threshold at the gray level θ ($1 \leq \theta \leq K$) was defined as follows:

$$\sigma_B^2(\theta) = \frac{[\mu_T \omega(\theta) - \mu(\theta)]^2}{\omega(\theta)[1 - \omega(\theta)]}, \quad (8)$$

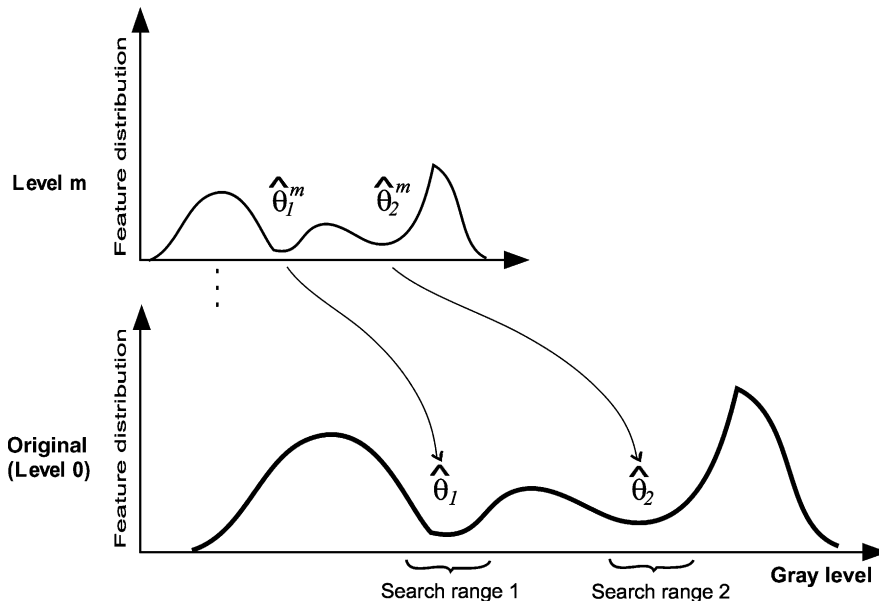


Fig. 2. Expansion to the original space.

where

$$\omega(\theta) = \sum_{i=1}^{\theta} h(i), \quad (9)$$

$$\mu(\theta) = \sum_{i=1}^{\theta} ih(i), \quad (10)$$

$$\mu_T = \sum_{i=1}^K ih(i). \quad (11)$$

The optimal threshold θ^* is determined as the following:

$$\theta^* = \max_{1 \leq \theta \leq K} \sigma_B^2(\theta). \quad (12)$$

The expansion modes are illustrated in Fig. 2 when two threshold values are desired.

(4) The given image is partitioned into multiple segments by the final optimal values θ_i .

The suggested algorithm is fast because we have decreased the search range for obtaining the optimum threshold values using MRA and a wavelets transform.

3. Experiments

We have applied the proposed scheme to several still images to verify the segmentation performance. Otsu's (1979) separability ($\sigma_B^2(\theta)$) was used to select the optimum threshold values θ_i based on the gray level distribution. However, there are many methods that use the distribution of features, such as the intensity and color (Pun, 1981; Abutaleb, 1989; Wu et al., 1999; Cao et al., 2002).

We consider two aspects to illustrate the reliability and feasibility of the devised algorithm. These are the processing time of the CPU for obtaining the final optimum threshold values θ_i , and the error rate of the segmentation result when the direct expansion values $\hat{\theta}_i$ are used to partition the given image.

An image segmentation approach based on the intensity distribution and spatial multi-resolution are introduced and compared with the performance of the proposed algorithm.

3.1. Processing time for optimal segmentation

In the proposed algorithm, three steps are checked for computation of CPU-time as follows:

- (1) The original signal is converted by level m wavelet transform. In this study, 'db1' wavelet and scaling signals are used.
- (2) A search procedure for θ_i^m in trend signal $h_A^m(l)$ at the lower resolution m .
- (3) Expansion to the original distribution $h(k)$ using the refinement mode and selection of the final optimum threshold values θ_i .

The final optimal threshold values θ_i are determined in the dynamic range where the gray level exists (Otsu, 1979). Thus, the search time becomes CPU-time for comparison with the proposed algorithm. We implemented our algorithm on a Pentium-III CPU at 700 MHz and Matlab 6.1.

For selection of a single threshold, the time consumed with the level of the wavelets transform is shown in Table 1. The second column displays the consumed CPU-time of Otsu's method where the final optimum threshold value θ_1 is determined

Table 1
CPU-time for selection of a single threshold (unit: ms)

Contents	Original space	Level 1 space	Level 2 space	Level 3 space
Lena	0.541	0.230	0.080	0.050
Airplane	0.430	0.140	0.071	0.050
Peppers	0.440	0.130	0.070	0.040
Boats	0.431	0.130	0.060	0.040
Claire	0.431	0.130	0.061	0.041

Table 2
CPU-time for selection of three thresholds (unit: ms)

Contents	Original space	Level 1 space	Level 2 space	Level 3 space
Lena	0.880	0.260	0.080	0.050
Airplane	0.982	0.271	0.081	0.050
Peppers	0.881	0.240	0.071	0.040
Boats	0.821	0.220	0.070	0.040
Claire	0.811	0.210	0.060	0.041

in the dynamic range where the gray level exists. The CPU-time of the proposed algorithm is shown in the three right columns of Table 1.

The proposed scheme is faster than Otsu's method in the original feature space (full space) even though a wavelets transform, search, and refinement procedures are added (Table 1). Greater speed is obtained due to reduction of dimension in the feature space by the wavelets transform. To obtain the same optimum threshold value, we can see that the consumed CPU-time is increased by a factor of approximately 10 in the case of level 3 transform (Table 1).

Since applications in computer vision and image processing require segmentation of an image into several regions, we tested our algorithm for multiple threshold selection (Table 2). When Otsu's search was performed in the original space, the consumed CPU-time increased two times because three thresholds ($\theta_1, \theta_2, \theta_3$) were examined. For the proposed scheme at the level 1 transformed feature space, the CPU-time was four times faster than the search time of Otsu's method. When a level 3 transform for the reduced-dimension feature space was used, the consumed time for segmentation was decreased by a factor of approximately 20 while the optimum thresholds ($\theta_1, \theta_2, \theta_3$) were same as those of Otsu's method in the original feature space.

The proposed scheme based on a wavelets transform and MRA is effective for image segmentation and real-time processing in computer vision applications. If the direct expansion mode without the refinement procedure is used, the required time is significantly decreased.

3.2. Segmentation performance

We verified the performance of segmentation results. Segmented results by the direct expansion values $\hat{\theta}_i$ were compared with results of the optimum threshold values θ_i . The error rate (ER) of the segmented result was simply defined as the ratio of the number of error pixels to the number of total pixels.

Tables 3 and 4 show the performance of segmentation results. The second column gives the optimum threshold value by Otsu's method. The direct expanded values and error rates are shown in the three right columns. From these results, the error rate increases as the level of the transform are increased, indicating that the trend signal is coarser than the original distribution as a wavelets transform is constructed for the lower resolution. However, the error rates are as low as 0–1.7% (Table 3).

With selection of multiple thresholds the error rate increases in comparison with the case of a

Table 3
The error rate for selection of a single threshold (unit: %)

Contents	θ_1	Level 1 space ($\hat{\theta}_1$)	Level 2 space ($\hat{\theta}_1$)	Level 3 space ($\hat{\theta}_1$)
Lena	117	0.531(116)	0.531(116)	1.700(120)
Airplane	154	0.000(154)	0.482(152)	0.480(152)
Peppers	120	0.000(120)	0.000(120)	0.000(120)
Boats	93	0.270(92)	0.270(92)	0.840(96)
Claire	81	0.064(82)	0.078(80)	0.078(80)

Table 4
The error rate for selection of three thresholds (unit: %)

Contents	θ_i	Level 1 space ($\hat{\theta}_i$)	Level 2 space ($\hat{\theta}_i$)	Level 3 space ($\hat{\theta}_i$)
Lena	77, 117, 166	0.90(76, 116, 166)	2.60(80, 116, 164)	3.7(80, 120, 168)
Airplane	101, 154, 195	1.70(102, 154, 194)	2.30(100, 152, 196)	5.1(104, 152, 192)
Peppers	65, 120, 166	0.34(66, 120, 166)	2.40(68, 120, 164)	3.6(72, 120, 168)
Boats	50, 93, 140	0.27(50, 92, 140)	0.60(52, 92, 140)	6.8(56, 92, 144)
Claire	38, 81, 182	0.48(40, 82, 182)	0.59(40, 80, 184)	0.5(40, 80, 184)

single threshold selection. Although this situation occurs in level 2 transformed space, the error rate is small whereas the consumed CPU-time for selection of thresholds can be decreased by a factor of 10 in comparison with Otsu's exhaustive search in the original distribution. That is, there exists a trade off between the CPU-time and the accuracy of the segmentation result.

Figs. 3 and 4 show the results of segmentation. The values in the parentheses denote the selected threshold values. There is little visual degradation of the quality of the segmented results. These results show that the error rates, which are shown in Tables 3 and 4, can be visually negligible.

Fast versions of feature distribution-based thresholding are given in (Wu et al., 1999; Cao et al., 2002). If we use these techniques for image segmentation, the consumed CPU-time can be reduced even more.

3.3. Comparison with spatial multi-resolution analysis

Image segmentation methods using multi-resolution analysis (MRA) have been reported for many years. Most methods focus on reduction of the amount of spatial data (Salgado et al., 2000; Shi and Shibasaki, 1999; Liapis et al., 2000; Noda et al., 2000; Acharyya and Kundu, 2001; Zhang and Oe, 1998; Charalampidis and Kasparis, 2002; Kim and Kim, 2003). These methods approximate the original image by spatially decomposition to a lower resolution. To compare these methods with the performance of our method, we considered an image thresholding method based on (1) spatial decomposition, (2) generation of the intensity distribution of the decomposed trend image in the

lower resolution, and (3) optimum threshold selection by the computed distribution. In this approach, there is no decomposition of the intensity distribution. This is herein referred to as spatial multi-resolution analysis (SMRA). The consumed CPU-time for threshold selection and the error rate of the segmentation result were determined using Otsu's criterion.

Tables 5–8 show the time required and the error rates for each method. For a single threshold selection, the proposed algorithm is slower than the SMRA because most of the processing time is used to generate the histogram of the image. In the proposed algorithm, the histogram is constructed from the original image whereas the SMRA method constructs the histogram from the decomposed image in the lower resolution. This is the main factor that causes the SMRA method to run faster than the proposed method. In viewpoint of the error rates from Table 7, we make sense that the proposed method gives the better results under the segmentation results by Otsu's full search are given as the ground-truth.

Both performance measures are better for the proposed algorithm in selection of multiple thresholds (Tables 7 and 8). A large segmentation error appears in the SMRA method (Table 8). Segmentation results are shown in Fig. 5. Visually, results from the SMRA method differ greatly from results of Otsu's full search. However, the proposed algorithm causes little degradation of the visual quality in comparison with segmentation results by Otsu's full search.

To evaluate objectively the performance of the proposed algorithm, we employ the Goodness function (G) by Liu and Yang (1994). This function was defined as the following:

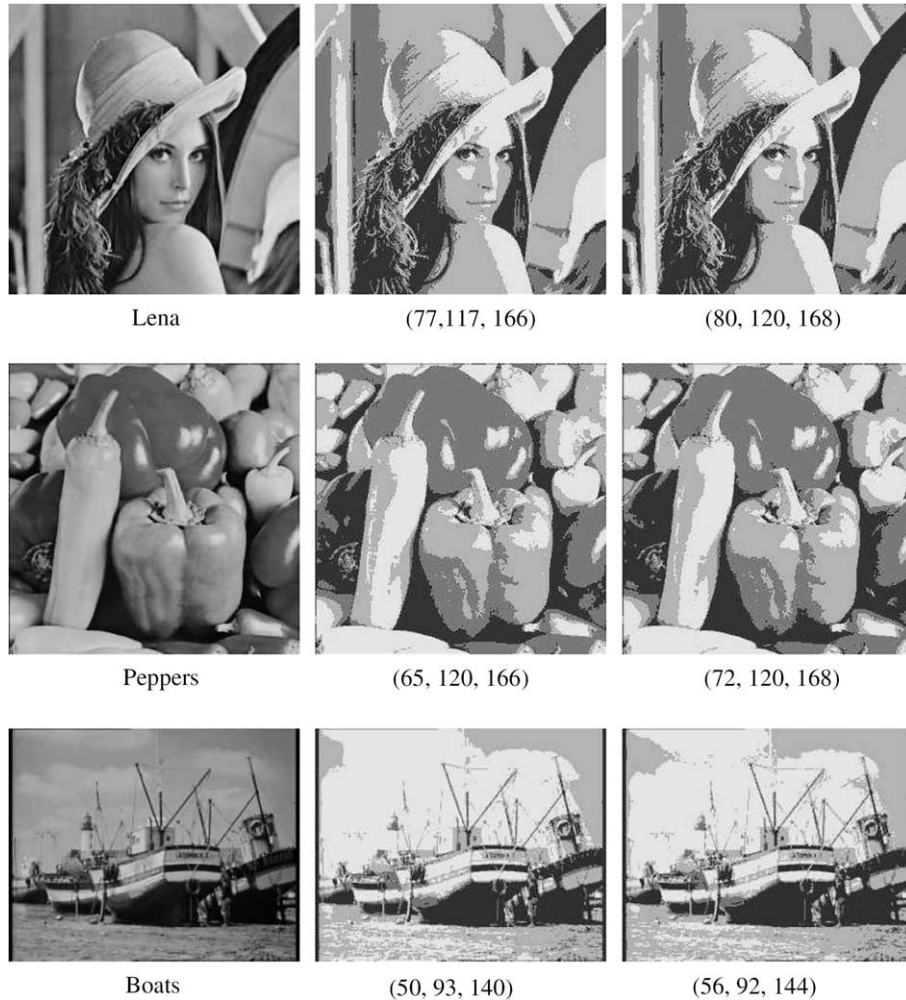


Fig. 3. Segmentation results for selection of three thresholds: the first column – originals, the second – results by Otsu's method in original feature space, the last – results by the direct expansion mode and level 3 wavelets transform.

$$G(I) = \sqrt{M} \times \sum_{i=1}^M \frac{e_i^2}{\sqrt{A_i}}, \quad (13)$$

where M is the number of regions in the segmented image, A_i is the number of pixels in the i th region, and e_i is the sum of the Euclidean distance of the color vectors/intensities between the original image and the segmented image in the i th region. Eq. (13) is composed of two terms: the first term, \sqrt{M} , penalizes segmentation that forms too many regions. The second term $e_i^2/\sqrt{A_i}$ is a local measure which penalizes small regions or regions with a

large color/intensity error since e_i indicates whether or not a region is assigned an appropriate color/intensity. In this paper, G is scaled down by the factor 1/10. The smaller value of G , the better is the segmentation result. In this comparison, the second term makes an effect on the performance evaluation only because the number of regions of the proposed algorithm are the same as that of the SMRA method.

Table 9 shows the Goodness of the segmented images for three thresholds selection. In the Lena and Airplane images, the proposed algorithm

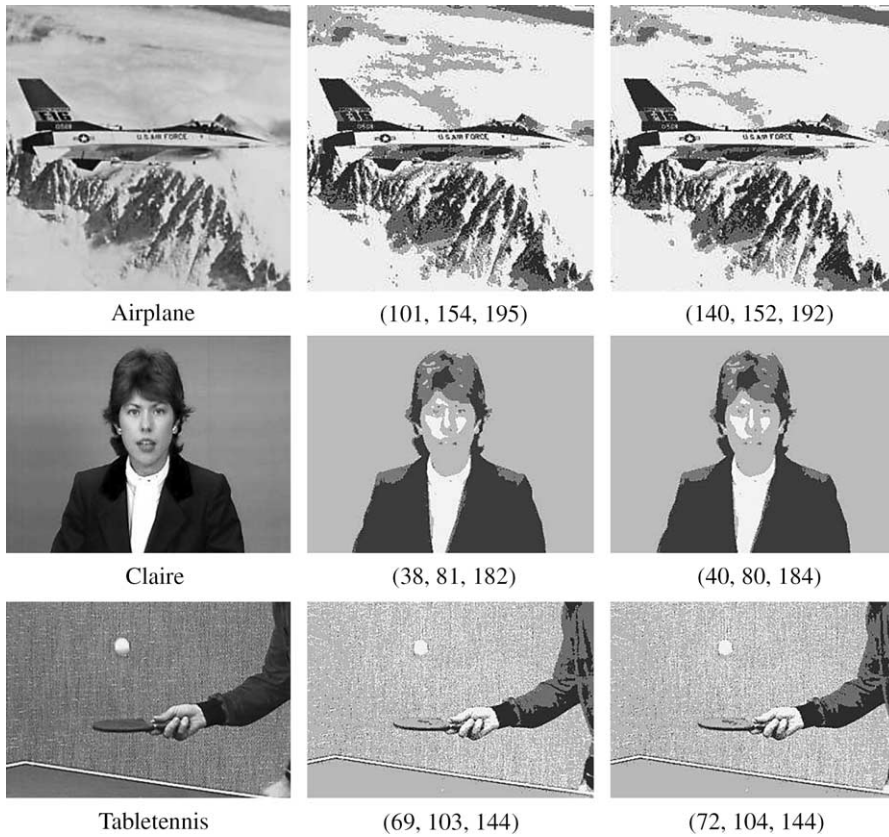


Fig. 4. Segmentation results for selection of three thresholds (continued).

Table 5
Performance comparison with the SMRA for a single threshold: CPU-time (unit: ms)

Contents	Level 1 space	Level 2 space	Level 3 space
Lena			
SMRA	0.93	0.71	0.66
Proposed	1.32	1.24	1.23
Airplane			
SMRA	0.88	0.70	0.67
Proposed	1.31	1.25	1.24
Peppers			
SMRA	0.89	0.71	0.67
Proposed	1.32	1.25	1.23
Boats			
SMRA	0.78	0.62	0.61
Proposed	1.07	1.01	0.98

Table 6
Performance comparison with the SMRA for three thresholds: CPU-time (unit: ms)

Contents	Level 1 space	Level 2 space	Level 3 space
Lena			
SMRA	1.93	1.48	1.41
Proposed	1.33	1.26	1.24
Airplane			
SMRA	1.97	1.53	1.49
Proposed	1.33	1.27	1.25
Peppers			
SMRA	1.80	1.49	1.44
Proposed	1.34	1.27	1.24
Boats			
SMRA	1.62	1.38	1.35
Proposed	1.09	1.01	0.99

Table 7

Performance comparison with the SMRA for a single threshold: the error rates (unit: %)

Contents	θ_i	Level 1 space ($\hat{\theta}_1$)	Level 2 space ($\hat{\theta}_1$)	Level 3 space ($\hat{\theta}_1$)
Lena				
SMRA	117	10.13(130)	13.38(134)	20.64(143)
Proposed		0.531(116)	0.531(116)	1.700(120)
Airplane				
SMRA	154	4.22(172)	6.00(178)	8.41(184)
Proposed		0.000(154)	0.482(152)	0.480(152)
Peppers				
SMRA	120	6.52(136)	9.34(141)	10.54(143)
Proposed		0.000(120)	0.000(120)	0.000(120)
Boats				
SMRA	93	9.25(117)	11.06(120)	21.44(132)
Proposed		0.270(92)	0.270(92)	0.840(96)

Table 8

Performance comparison with the SMRA for three thresholds: the error rates (unit: %)

Contents	θ_i	Level 1 space ($\hat{\theta}_i$)	Level 2 space ($\hat{\theta}_i$)	Level 3 space ($\hat{\theta}_i$)
Lena				
SMRA	77, 117, 166	20.87(85, 130, 184)	26.71(89, 134, 189)	39.83(96, 143, 198)
Proposed		0.97(76, 116, 166)	2.60(80, 116, 164)	3.70(80, 120, 168)
Airplane				
SMRA	101, 154, 195	55.43(115, 172, 216)	66.26(125, 178, 220)	67.77(133, 184, 219)
Proposed		1.70(102, 154, 194)	2.30(100, 152, 196)	5.10(104, 152, 192)
Peppers				
SMRA	64, 120, 166	24.07(88, 136, 188)	32.51(79, 141, 192)	36.57(84, 143, 191)
Proposed		0.34(66, 120, 166)	2.40(68, 120, 164)	3.60(72, 120, 168)
Boats				
SMRA	50, 93, 140	54.71(61, 117, 173)	58.38(68, 120, 176)	70.38(75, 132, 180)
Proposed		0.27(50, 92, 140)	0.60(52, 92, 140)	6.8(56, 92, 144)

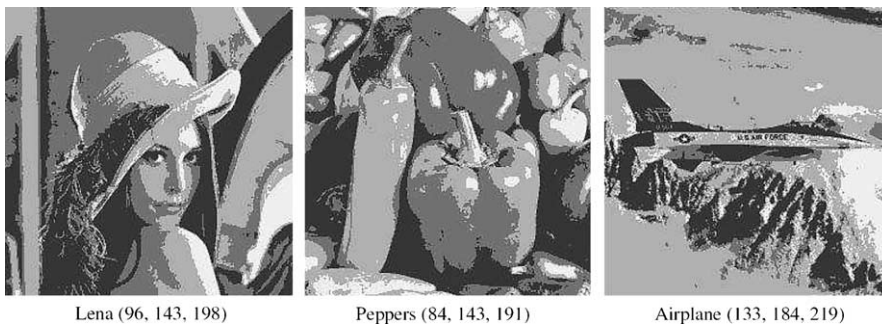


Fig. 5. Segmentation results for selection of three thresholds by the SMRA with level 3 wavelets transform.

Table 9
Performance comparison with the SMRA for three thresholds:
the Goodness function (G)

Contents	Level 1 space	Level 2 space	Level 3 space
Lena			
SMRA	1100.0	1120.0	1200.0
Proposed	1090.0	1100.0	1080.0
Airplane			
SMRA	989.0	998.3	997.3
Proposed	986.4	996.5	992.3
Peppers			
SMRA	1340.0	1420.0	1470.0
Proposed	1200.0	1200.0	1200.0
Boats			
SMRA	959.9	949.7	943.5
Proposed	841.2	841.2	845.3

makes a little improvement of the segmentation on the whole. Also, we make sense that the large improvement of the segmentation performance is made in the Peppers and Boats images. As a result, we can see that the proposed algorithm has ability to improve the segmentation performance although the consumed CPU-time for thresholds selection decreases.

4. Conclusion

We have proposed a fast technique for image segmentation based on a multi-resolution application of a wavelets transform and feature distribution. To derive fast computation of the optimum threshold values in a feature space, the original feature space is transformed into a lower resolution using a wavelets transform. Based on this lower resolution version of the given feature space, a single feature value or multiple feature values are determined as optimum threshold values. The optimum feature values, which are in the lower resolution, are then projected onto the original feature space. A refinement procedure may be added to detect optimum threshold values. Experimental results show the reliability and effectiveness of the proposed algorithm in view of the consumed CPU-time and the accuracy of segmentation.

We have described the performance of the proposed algorithm with a one-dimensional feature distribution. However, the proposed scheme will be more effective for a multi-dimensional feature distribution, such as two-dimensional entropy and three-dimensional color clustering. This scheme can also be adopted in many applications for data classification based on the feature distribution.

References

- Abutaleb, A.S., 1989. Automatic thresholding of gray-level picture using two-dimensional entropy. *Comput. Vision, Graphic, Image Process.* 47, 22–32.
- Acharyya, M., Kundu, M.K., 2001. Wavelet-based texture segmentation of remotely sensed images. *IEEE 11th Internat. Conf. Image Anal. Process.*, 69–74.
- Calvard, S., 1978. Picture thresholding using an iterative selection method. *IEEE Trans. Systems, Man, Cybernet.* 8 (8), 629–632.
- Cao, L., Shi, Z., Cheng, E.K.W., 2002. Fast automatic multilevel thresholding method. *Electron. Lett.* 38 (16), 868–870.
- Charalampidis, D., Kasparis, T., 2002. Wavelet-based rotational invariant roughness features for texture classification and segmentation. *IEEE Trans. Image Process.* 11 (8), 825–837.
- Goswami, J.C., Chan, A.K., 1999. *Fundamentals of Wavelets-theory, Algorithm, and Applications.* Wiley Inter-Science.
- Kim, J.B., Kim, H.J., 2003. Multiresolution-based watersheds for efficient image segmentation. *Pattern Recognition Lett.* (24), 473–488.
- Kittler, J., Illingworth, J., 1986. Minimum error thresholding. *Pattern Recognition* 19 (1), 41–47.
- Kumar, A., Bar-Shalom, Y., Oron, E., 1995. Precision tracking based on segmentation with optimal layering for imaging sensors. *IEEE Trans. Pattern Anal. Machine Intell.* 17 (2), 182–188.
- Liapis, S., Sifakis, E., Tziritas, G., 2000. Color and/or texture segmentation using deterministic relaxation and fast marching algorithms. *IEEE 5th Internat. Conf. Pattern Recognition* 3, 617–620.
- Liu, J., Yang, Y.-H., 1994. Multiresolution color image segmentation. *IEEE Trans. Pattern Anal. Machine Intell.* 16, 689–700.
- Noda, H., Shirazi, M.N., Kawaguchi, E., 2000. Textured image segmentation using MRF in wavelet domain. *IEEE Internat. Conf. Image Process.* 3, 572–575.
- Otsu, N., 1979. A threshold selection method from grey-level histograms. *IEEE Trans. Syst. Man Cybernet. SMC-9* (1), 62–66.
- Pun, T., 1981. Entropic thresholding, a new approach. *Comput. Graphics Image Process.* 16, 210–236.

- Salgado, L., Garcia, N., Menéndez, J.M., Rendón, E., 2000. Efficient image segmentation for region-based motion estimation and compression. *IEEE Trans. Circuit Syst. Video Technol.* 10, 1029–1039.
- Shi, Z., Shibasaki, R., 1999. An approach to image segmentation using multiresolution analysis of wavelets. *IEEE Internat. Conf. Syst., Man, Cybernet.* VI, 810–815.
- Walker, J.S., 1999. *A primer on wavelets and their scientific applications*. Chapman & Hall/CRC.
- Wu, X.J., Jhang, Y.J., Xia, L.Z., 1999. A fast recurring two-dimensional entropic thresholding algorithm. *Pattern Recognition* 32, 2055–2206.
- Zhang, J., Oe, S., 1998. Texture image segmentation method based on wavelet transform and neural network. *Proc. IEEE Internat. Conf. Syst., Man Cybernet.* 5, 4595–4600.